

Identifying Areas of High Gold Potential Using Geochemical Prospecting Methods: The Tenado Area in the Boromo Birimian Belt, West-Central Burkina Faso, West Africa

Aziz Fayçal Tarnagda

Laboratoire Géosciences et Environnement (LaGE), Earth Sciences
Department, Ouagadougou, Burkina Faso
University Joseph KI ZERBO (UJKZ), Ouagadougou, Burkina Faso

Pascal Ouiya

Laboratoire Géosciences et Environnement (LaGE), Earth Sciences
Department, Ouagadougou, Burkina Faso
Ecole Normale Supérieure (ENS), Institute of Science and Technology
(IST), Ouagadougou, Burkina Faso

Saga Sawadogo

Laboratoire Géosciences et Environnement (LaGE), Earth Sciences
Department, Ouagadougou, Burkina Faso
University Joseph KI ZERBO (UJKZ), Ouagadougou, Burkina Faso

[Doi:10.19044/esj.2024.v20n2p191](https://doi.org/10.19044/esj.2024.v20n2p191)

Submitted: 22 October 2023

Accepted: 30 January 2024

Published: 31 January 2024

Copyright 2024 Author(s)

Under Creative Commons CC-BY 4.0

OPEN ACCESS

Cite As:

Tarnagda A.F., Ouiya P. & Sawadogo S. (2024). *Identifying Areas of High Gold Potential Using Geochemical Prospecting Methods: The Tenado Area in the Boromo Birimian Belt, West-Central Burkina Faso, West Africa*. European Scientific Journal, ESJ, 20 (2), 191.

<https://doi.org/10.19044/esj.2024.v20n2p191>

Abstract

The investigation area is located in the central-western region of Burkina Faso, in a geological environment that incorporates the Paleoproterozoic formations of the Boromo greenstone belt. This zone already has several gold showings and an active zinc mine, but no major gold deposits. The aim of this study is to define target areas with high gold potential for further prospecting. To meet this objective, we mainly used total rock geochemistry and stream sediment geochemistry methods. The combination of stream sediment gold content and litho-geochemical data has enabled us to highlight two areas of gold (Au) and various metal anomalies. The gold

content of stream sediments is mainly influenced by that of the parent rock from which they are derived. In fact, strong gold anomalies are more common in clay sediments than in sandy sediments. These clay sediments are derived from basic rocks (basalt) and intermediate rocks (andesite-dacite), while the gold-poor sandy sediments are derived from granitoids. Basic to intermediate rocks are fertile for primary gold. Anomaly zone one (01) in the northern part of the study area (Kelsio, Zoula, Poa and Dyoro) and anomaly zone two (02) in the southern part of the study area (Kwademan, Baguiomo, Bérédo, Bonga and Baganapou) show occurrences of mainly gold and various metals (Zn, Cu, Ni).

Keywords: Anomaly area, Paleoproterozoic, Boromo Birimian Belt, Burkina Faso

1. Introduction

Many studies of the West African craton have shown that it is rich in metal mineralization (Milési et al., 1989, 1992; Groves et al., 1998; Markwitz et al., 2016; Goldfarb et al., 2017; Masurel et al., 2021). This craton is made up of two major dorsals: the Reguibat dorsal to the north and the Man/Leo dorsal to the south. In the Man/Leo Ridge, Archean formations lie to the east and Paleoproterozoic formations to the west (Fig.1-A). The Paleoproterozoic formations in this western part of the dorsal are still called Birimian formations (Kitson, 1918; Junner, 1940; Bonhomme, 1962; Bessoles, 1977) and are affected by the Eburnian orogeny (Feybesse et al., 2006). These Birimian formations consist of alternating greenstone belts cut by different generations of granitoids (Hirdes et al., 1996; Doumbia et al., 1998; Gasquet et al., 2003; Baratoux et al., 2011; Ganne et al., 2014).

Most orogenic gold deposits in the Man/Léo dorsal and particularly in Burkina Faso are contained in greenstone belts (Castaing et al., 2003; Giovenazzo et al., 2018). In view of the mining potential offered by these Birimian volcano-sedimentary belts, we turned our attention to the Boromo greenstone belt, which is already known for its gold and base metal potential.

Today, geochemical prospecting is increasingly used in mineral exploration to detect and delineate areas of geochemical anomalies of one or more metals (Carranza, 2010; Yousefi et al., 2013; Abdolmaleki et al., 2014; Darehshiri et al., 2015; Shine et al., 2022). There are several methods of geochemical investigation, depending on the element to be investigated. These include litho-geochemistry, soil geochemistry and stream sediment geochemistry for metal detection. Although stream sediment geochemistry can be used to search for metal anomalies, this type of sample remains transported, and it is imperative to involve other geochemical prospecting methods such as litho-geochemistry. Indeed, the difficulty in analyzing stream

sediment data lies in determining the source from which it originates (Ndome Effoudou-Priso et al., 2014; Sorokina, 2019; Noa Tang et al., 2020). The availability of outcropping rock samples near stream sediment sampling points for litho-geochemical analysis would be a major asset in delineating areas with high gold potential.

This study is carried out in the central-western region of Burkina Faso, which was the subject of a geochemical prospecting study in 1982. This work led to the discovery of the Perkoa Zn-Ag sulphide cluster deposit (Franceschi and Ouédraogo, 1982). Since then, other initiatives have followed (Kabore et al., 1989), but to date no major gold (Au) deposit has been discovered in the area. The aim of this work is to delineate zones of interest with high gold potential in the Central West region, in order to guide future prospecting with a view to discovering a large gold deposit. To achieve this, we used stream sediment data and total rock geochemistry (litho-geochemistry). We discuss the origin of gold in stream sediments.

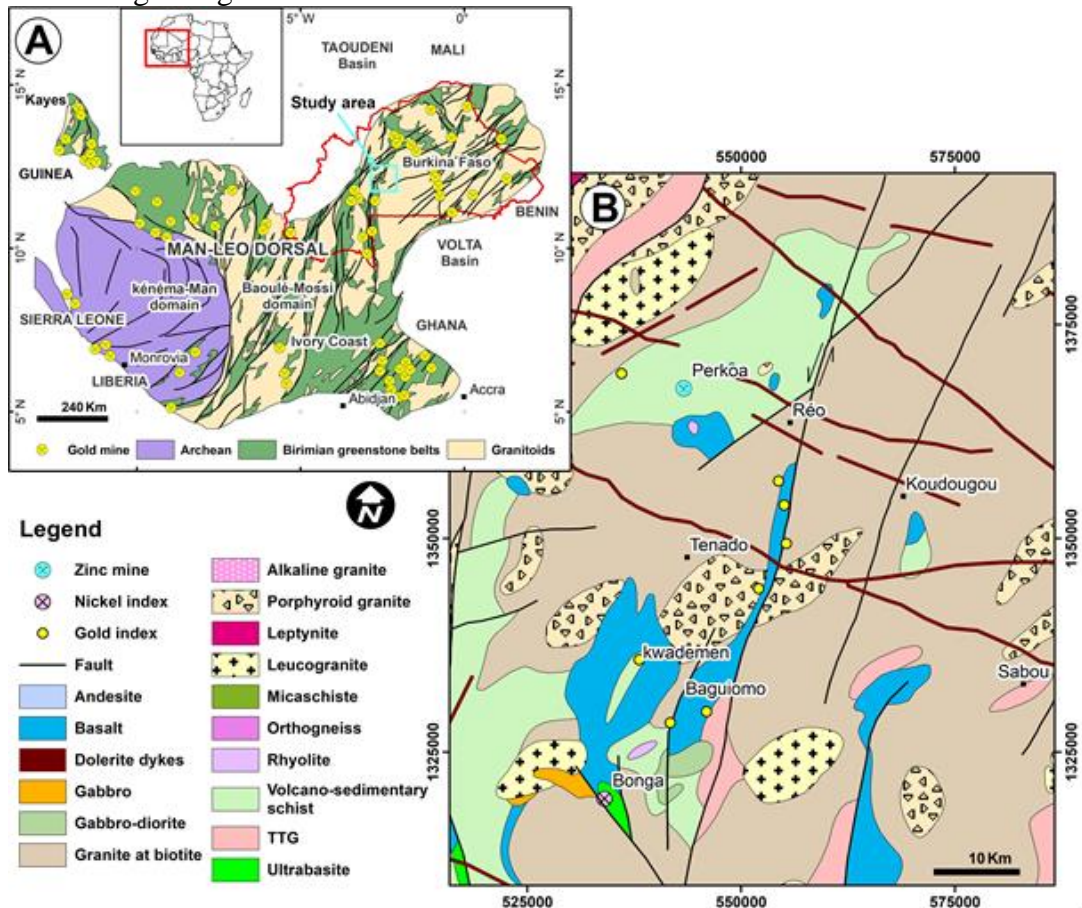


Figure 1. (A) Modified litho-structural and metallogenic map of the Léo dorsal, after Milesi et al. (2004) and (B) Synthesis geological map of Burkina Faso, modified after Castaing et al. (2003).

2. Regional geological context

The geology of the central-western region is dominated by granitoids and the volcano-sedimentary formations of the Boromo greenstone belt (Fig.1B). The combination of granitoids and volcano-sedimentary belt is late cut by dolerite dykes (Castaing et al., 2003; Dahl et al., 2018). The portion of the Boromo greenstone belt that crosses the study area in the Tenado commune is composed of volcanic rocks, volcano-sedimentary rocks and sedimentary rocks.

The volcanic series is composed of basalt, andesite, dacite and rhyolite. There is also the presence of ultrabasite, most often associated with gabbros (Béziat et al., 2000). The sedimentary formations include metagrites, tuffaceous schists, sericite schists and manganiferous black schists (Schwartz and Melcher, 2003; Chevremont et al., 2003). Intercalations of gabbros, Rhyolites, dolerites and diorites are found throughout the volcano-sedimentary package. These assemblages are organized into greenstone belts by two generations of granitoids in the study area, The first generation is represented by the TTG (Tonalite Trondhjemite Granodiorite) series, which outcrops mainly in the extreme NW and SE of the study area, Their emplacement locally induces amphibolite-facies metamorphism at the contacts with the Boromo greenstone belt formations (Chevremont et al., 2003). The second generation, consisting of biotite granite, porphyritic biotite granite and leucogranite, outcrops throughout the study area (Chevremont et al., 2003; Ouedraogo et al., 2003). All these formations are later cut by NW-SE trending dolerite dykes. Structurally, three deformation phases (D1 to D3) are accepted (Feybesse et al., 1990 ; Baratoux et al., 2011; Metelka et al., 2011). The first phase of deformation (D1) is marked by a general NW-SE shortening and oriented the greenstone belt in a N-S to NE-SW direction. The second deformation phase (D2) is characterized by predominantly sinister shear zones, followed by the final deformation phase (D3). The structures of D3 are of the type : steeply dipping crenulation cleavage, trending E-W on average, and reverse faults dipping shallowly to the north or south. These deformation structures have given rise to a number of hydrothermal deposits in the central west, including the Zn-Ag volcanogenic sulfide cluster (VMS) polymetallic deposit at Perkoa and the Kwademen gold deposit.

3. Methodology

Total rock geochemistry sampling was carried out on outcrops observed during the mapping phase on a regional scale of 1:200,000. The rocks sampled were conditioned at the BUMIGEB (Bureau of Mines and Geology of Burkina Faso), then underwent treatments ranging from crushing to grinding. The powders obtained from this process are pulverized, sieved to a fine mesh of around 75 microns and then digested with acid (aqua regia) for

at least an hour in a graphite heating block. After cooling, the resulting solution is diluted to 12.5 ml with demineralized water, mixed and analyzed by inductively coupled plasma-atomic emission spectrometry (ICP-AES). In all, we acquired 32 results from these analyses, which are expressed as a percentage of oxide weight for major elements and in ppb (part per billion) for trace elements and the various metals analyzed (Au, Ag, Zn, Ni, Cu, etc.).

In addition to these total rock geochemistry data, we also used stream sediment data, numbering 284 stream sediment analysis results. As far as stream sediments are concerned, the work was carried out on a regional scale, with several samplings of fine material (1 to 3 kg) deposited in river beds or on banks. The sampling grid is 10 km, i.e. four samples per km². These samples were sieved in the BUMIGEB laboratory to a mesh size of 63 µm and then sent for ICP AES analysis to the BRGM laboratory in Orleans, France. The detection limit in these analyses is of the order of 1 ppb. The geochemical anomaly area delineation method used in this work is the iso-tenor or iso-contour delineation method. It was carried out in ArcMap 10.8 mapping software using the geostatistical interpolation method based on the Kriging technique.

4. Results

4.1 Spatial distribution of chemical anomalies

The spatial distribution of gold grades in the stream sediment results shows several anomalous gold zones that stand out due to their high concentrations. Most of the high gold grades are isolated and distributed along the banks of the various rivers (Mouhoun, Nazinon and Sissili) drained by their watersheds, with a topography that varies widely in altitude (240 to 480 m), resulting in significant alluvial input (Fig.2A).

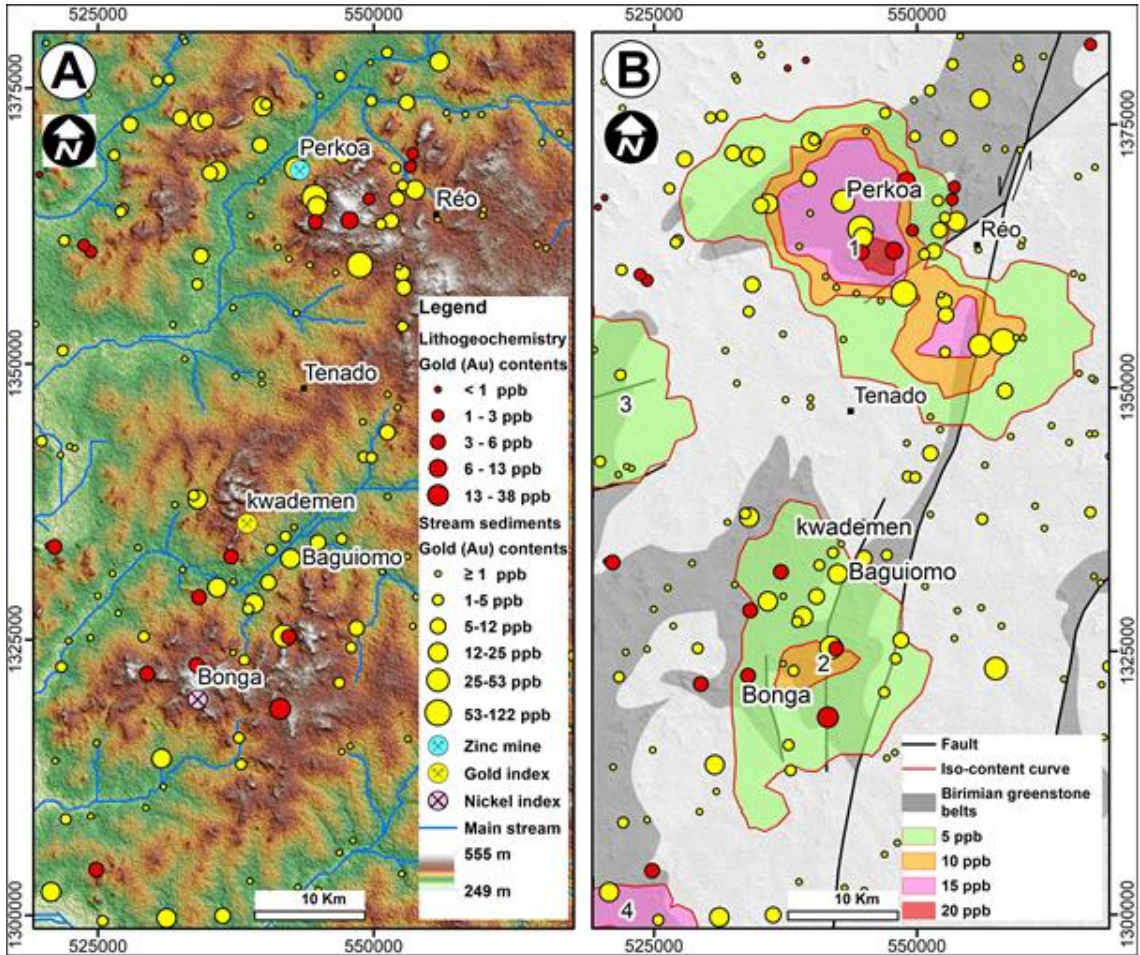


Figure 2. A) Map showing the distribution of gold grades from river sediments and litho-geochemical data against the background of the Digital Elevation Model (DEM). B) Map of delineated Au anomaly zones.

Analytical data from stream sediments show two (2) major gold (Au) anomaly areas (Fig.2B). Most of the four anomaly areas are located in the Boromo greenstone belt. Within these four zones, two (2) anomaly areas stand out from the rest, namely anomaly areas 1 and 2 respectively located in the vicinity of the Perkoa mine and the Kwademen artisanal mine by their high grades of certain elements such as: Au, Zn, Cu and Ni (Table I).

Table I. Anomaly zone 1 and 2 stream sediment data table

Samples	OA482	SR388	OA480	SM408	OA489	SR385	OA491	SR436	SM329	SR384	YI036	SM324	YI040	SM328	KS9	KS13	SM383	SM387	SM391	KS11	OA452	SM381	SM385	OA450	JG7	JG3	JG5	OA448	JG9
Anomaly	Zone 1	Zone 2																											
Material	clayey																												
Long	-2.59	-2.53	-2.59	-2.63	-2.67	-2.52	-2.63	-2.68	-2.52	-2.52	-2.6	-2.46	-2.49	-2.51	-2.66	-2.65	-2.63	-2.65	-2.67	-2.65	-2.61	-2.61	-2.64	-2.61	-2.62	-2.55	-2.56	-2.63	-2.57
Lat	12.35	12.33	12.34	12.42	12.37	12.35	12.39	12.41	12.29	12.37	12.37	12.21	12.25	12.27	11.97	11.91	12.03	12.01	12.03	11.97	12.08	12.05	12.02	12.07	11.99	11.99	11.98	12.06	11.95
Majors elements (wt%)																													
SiO ₂	50.5	52.2	59.9	60.3	62	62.5	63.7	63.7	63.8	66	66.5	76.7	76.7	78.5	46.6	51.7	59	59.1	59.1	60	61.1	61.4	61.4	62.7	63.4	65.4	65.5	79.3	79.9
Al ₂ O ₃	14.7	16.1	11.9	12.9	12.8	10.8	12.7	13.8	12.4	10.7	9.3	10.8	9.6	11.2	20	16	15.8	16.3	15.2	13.6	12.6	12.4	12.6	12	11	11	11.7	10.5	8.7
Fe ₂ O ₃	8.2	8.6	7.6	6	4.3	5.7	5	3.9	6.2	5.5	5.5	4.2	6.3	3.9	9.7	6.6	6.8	3.8	5.7	6	5.9	5.6	6.1	6	6.4	5.7	5.8	3.5	1.7
CaO	2.6	1.1	2.4	1.4																1.8		1.5	1.4		2.2	1.1	1.3		
K ₂ O	0.8	1.1	0.7	0.8	1.1			1.3	0.9	0.8	0.9	1	0.7	0.9	1.2	1.1	1	1.2	1.3	0.9	0.9	0.9	1	0.9	0.6	0.8	0.8	1	0.8
MnO	0.23	0.17	0.15	0.09	0.13	0.11	0.08	0.05	0.12	0.09	0.06	0.07	0.07	0.08	0.13	0.09	0.1	0.07	0.15	0.06	0.13	0.06	0.07	0.17	0.09	0.07	0.07	0.08	0.04
TiO ₂	1.08	1.69	1.16	1.16	1.42	1.44	1.23	1.34	1.24	1.52	1.25	1.17	1.55	1.34	1.31	1.32	1.32	1.46	1.38	1.08	1.38	1.27	1.3	1.18	1.2	1.18	1.23	1.19	1.18
Au (ppb)	9	4.5	15.3	16.2	15.3	5.6	6.8	6.1	8.4	4.3	37.7	7.7	38	7.8	1	3.3	8.8	1.5	24.2	4.2	1	16.9	13.6	4.4	30.7	5.3	4.7	4.4	2.8
Traces elements (ppm)																													
Co	48	36	34	25	20	25	21	16	25	28	18	18	18	16	31	31	23	19	33	17	27	17	21	28	18	13	13	16	8
Ni	70	79	56	76	34	42	48	38	38	56	30	30	31	32	135	282	68	43	55	54	40	56	79	48	68	47	49	37	23
Cu	76	83	81	41	31	54	34	28	58	60	50	34	41	23	58	42	61	34	52	55	38	50	54	40	51	43	42	30	21
Zn	80	99	66	59	52	55	60	49	68	58	43	40	41	39	82	52	61	59	62	41	63	50	60	64	42	40	43	35	20
Y	39	57	40	39	48	44	41	45	40	34	44	42	39	47	46	46	41	52	46	33	52	38	38	42	30	31	32	37	46
Nb	20	32	23	26	31	28	26	34	26	21	20	31	22	38	26	31	27	39	29	21	33	26	25	26	22	26	24	30	33
Ba	414	332	272	323	443	359	471	455	305	267	269	388	237	348	438	387	414	502	539	356	372	345	378	379	220	261	295	409	272
La	30	43	27	40	55	32	40	50	34	22	27	44	25	47	47	53	45	69	50	29	53	33	34	37	21	26	26	40	41
Ce	58	66	45	64	92	53	68	79	59	36	67	87	63	99	72	87	59	122	86	41	97	41	48	67	27	36	36	67	78
Pb	10	18	10	17	15	13	<10	17	13	10	19	20	14	19	13	12	13	22	16		26	11	12	23				21	
Al ₂ O ₃ /TiO ₂	13.61	9.53	10.26	11.12	9.01	7.5	10.33	10.3	10	7.04	7.44	9.23	6.19	8.36	15.27	12.12	11.97	11.16	11.01	12.59	9.13	9.76	9.69	10.17	9.17	9.32	9.51	8.82	7.37
SiO ₂ /Al ₂ O ₃	3.44	3.24	5.03	4.67	4.84	5.79	5.02	4.62	5.15	6.17	7.15	7.1	7.99	7.01	2.33	3.23	3.73	3.63	3.89	4.41	4.85	4.95	4.87	5.23	5.76	5.95	5.6	7.55	9.18
Cr/Ni	2.24	1.7	2.21	2.62	2.21	2.19	2.02	2.42	2.13	1.63	2.83	2.03	2.23	1.94	1.3	1.16	2.15	2.07	1.96	2.46	1.68	2.07	2.47	1.56	2.56	2.3	2.57	1.89	2.35

Overall, it can be seen that stream sediment samples, mainly of the clay type, are the most mineralized in Au, Cu, Zn and Ni compared with sandy samples (Fig.03). In tropical environments, alteration of the mafic (basalt) to intermediate (andesite) formations of the greenstone belt will yield mainly clay samples. Whereas in granitic formations, feldspar and ferromagnesian minerals will tend to weather into clay (kaolinite, gibbsite etc.) and quartz, being highly resistant to weathering, will be associated with clays (sandy-clay material). In addition, these clays will disperse and, in the end, the quartz grains will concentrate to form essentially sandy material. Despite all this, it is difficult to establish a direct correlation between the origin of clays and the parent rock from which they are derived. Moreover, in terms of metal content, there is contamination linked to artisanal gold panning. As a result, the levels of various metals in stream sediments are often contrasted in relation to certain types of material sampled.

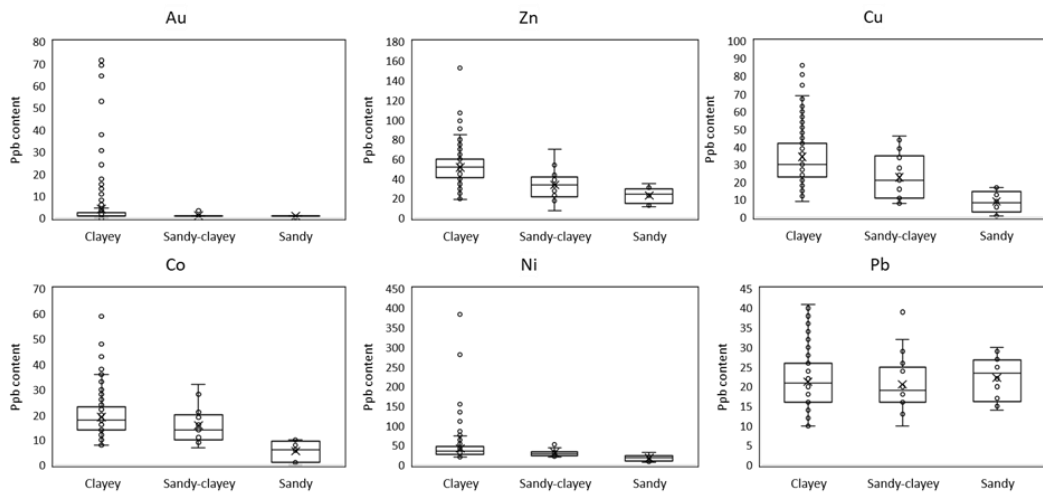


Figure 3. Moustache box of the distribution of various metals in stream sediments

The spatial distribution of gold (Au) grades from total rock geochemistry shows that anomaly areas 1 and 2 are zones of high gold potential (Fig.2B). Pearson correlation coefficients calculated from stream sediment data from anomaly zones 1 and 2 show an intercorrelation between certain metals (Table II). A strong correlation is observed between Ni-Cr and Cu-Co-Zn, while gold (Au) shows a weak correlation with Co, Cu and Zn.

Table II. Correlation matrix between metal contents from zone 1 and 2 stream sediment data (n= 53)

	Au	Co	Cr	Cu	Ni	Pb	Zn
Au	1	0.24	-0.04	0.18	-0.06	-0.15	0.08
Co		1	0.43	0.75	0.41	0.04	0.75
Cr			1	0.38	0.83	-0.11	0.32
Cu				1	0.32	-0.18	0.72

Ni	1	-0.15	0.31
Pb		1	0.25
Zn			1

Anomaly zone 1 (01), located in the Perkoa locality, has Cu values ranging from 1.76 to 326.31 ppb, followed by Ni, Zn and Au respectively, with values up to 112 ppb (Fig.4A). In zone one (01), a complex of Zn-Pb-Ag-Au anomalies has been described at the Perkoa zinc mine within the differentiated volcano-sedimentary formations of the greenstone belt (Kabore et al., 1989). In the second anomaly area (2), Ni levels stand out with values as high as 282 ppb (Fig.4B). Bouga is located within this zone, where nickel showings are reported in a set of Ni-Co-Cr anomalies resulting from peridotite alteration, extending over a small area (Kabore et al., 1989). Furthermore, in this zone (02) another set of Au-Cu-Ag anomalies has been reported at the Kwademen artisanal mine and has been described as related to quartz veins or silicified zones mineralized in sulfide and Au (Ouedraogo, 1988).

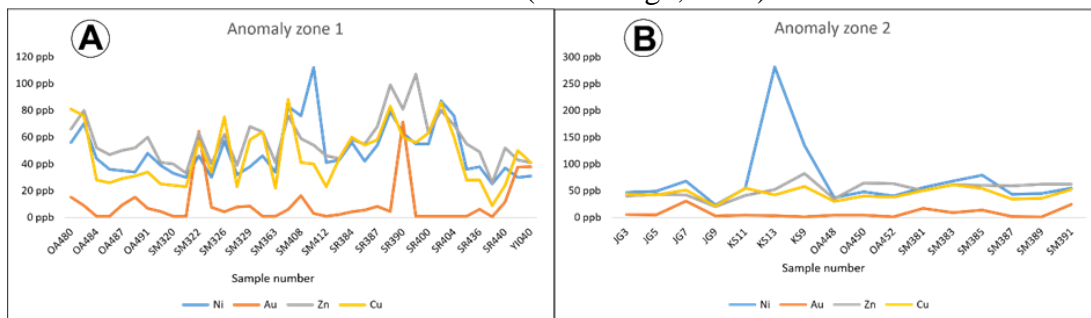


Figure 4. A) Gold grade distribution in Anomaly Zone 1;
B) Gold grade distribution in Anomaly Zone 2.

4.2 Geochemistry of volcanic units

The total rock geochemistry of the various volcanic units (Table III) reveals that the volcanic formations present in the study area range from basic to acidic in composition, passing through intermediate terms according to the TAS diagram (Middlemost, 1994) (Fig.5-A). These volcanic formations are essentially basalts, basaltic andesites, andesites, dacites and rhyolites. Basalt flows are characterized by variable SiO₂ contents ranging from 45.09 to 50.88% (Fig.5-A). In Jensen's (1976) diagram, basalts show an affinity for the iron-rich tholeiitic series, while andesites, dacites and rhyolites are placed in the calc-alkaline series (Fig.5-B). The geodynamic environment of these basalts lies within the mid-ocean ripple field (MORB) based on the diagram of Hollocher et al. (2012) and the calc-alkaline series formations lie within the island arc field (Fig.5-C).

Table III. Table of rock geochemistry data on volcanic formations

SAMPLE	E0092	MD0304	MD0321	MD0339	MD0381	MD0448	PC0297	JM0413	JM0427	JM0453	MD0340	MD034A	MD034B
Litho	Dacite	Andesite	Andesite	Basalte	Rhyolite	Epiclastite	Basalt	Ultrabasite	Basalt	Basalt	Basalt	Basalt	Basalt
Long	-2.5	-2.5	-2.7	-2.5	-2.6	-2.8	-2.2	-2.6	-2.7	-2.6	-2.48	-2.5	-2.63
Lat	12.4	12.3	12.1	12.4	12.3	12.1	12.3	11.9	12	12	12.27	12.38	12.07
TiO ₂	0.2	0.7	1.2	1.2	0	0.3	1.3	4.6	0.6	1.1	1.08	1.23	1.13
Al ₂ O ₃	15.3	15.8	14.7	15.2	13.8	10	17.2	61.7	13.7	14.2	14.3	15.33	14.32
Fe ₂ O ₃	3.1	6.4	11.5	12.9	0.6	3.1	10.4	1.3	9.6	12.7	12.68	11.84	12.16
MnO	0.1	0.1	0.2	0.2	0.1	0.1	0.2	0	0.2	0.2	0.2	0.19	0.2
MgO	0.7	4.2	3.8	5.5	0	0.3	5.5	0.2	3.8	4.5	6.81	6.73	3.09
CaO	3.8	5.1	8.5	12.4	0.5	0.9	9.7	4.7	13.6	13.1	10.58	11.74	16.46
Na ₂ O	5.4	3.4	3.2	1.4	4.7	2.3	2.9	0.6	1.3	1.3	1.94	2.19	0.45
K ₂ O	0.6	1.8	0.3	0.2	3.8	2	0.5	1.6	0.2	0.1	0.27	0.11	0.08
P ₂ O ₅	0.1	0.2	0.1	0.1	<0.01	0	0.2	<0.01	0.1	0.1	0.11	0.08	0.12
LOI	1.1	1.6	1.4	0.5	1.2	2.8	0.9	3.4	2.8	1.9	2.44	0.59	2.87
Total	98.9	98.4	98.6	99.5	98.8	97.2	99.1	96.6	97.2	98.1	97.56	99.41	97.13
Traces elements (ppm)													
Co	4.3	26.4	44.4	60.9	10.2	13.3	39	0	0	0	56	50.7	40.3
Cr	139	121	3	29	6	13	10	0	0	0	40	7	10
Ag	8	46	15	38	97	20	21	51	16	14	30	46	12
Au (ppb)	13	3	5	3	6	6	3	38	5	6	9	2	6
Cu	15.9	14.6	13	97.8	3.5	3.8	28	17.1	39.2	69	106.27	154	9.79
Mo	2.3	0.4	1.4	0.4	0.1	0.2	0.8	3.8	0.7	0.8	0.42	0.26	0.59
Pb	0.6	10.3	3.9	3.1	54.3	11.9	3.2	9.7	17.9	21.4	11.98	3.48	5.13
Zn	32.4	73	31	15.4	49.6	10.3	47.8	4.4	19.9	39	39.9	34.1	26.1
Ni	9	101.4	14.4	132.2	1.1	13.6	25.3	11.7	44	55.1	143.5	109.8	27.6
Nb	2.8	5.5	4.1	3.2	30.8	3	6.9	17.8	4.1	3.4	2.5	3.5	3.4
Th	1.3	3.4	1.7	0.2	17.4	4.6	0.7	3.5	1.4	0.5	0.3	0.3	0.8
La	10.6	21.4	12.6	4	6.3	28.8	11	33.6	11.4	6.7	4.5	3.8	7.9
Ce	20.7	43	24.2	9.9	12.9	47.4	25.1	54.4	22.9	9.4	11	10.4	15.9
Pr	2.4	5.2	3.1	1.6	1.6	5.9	3.3	7.9	3.2	2.1	1.71	1.5	2.4
Nd	8.5	21.3	13.8	8.9	6.2	21.6	15.3	34.6	13.9	10.3	9.2	8	11.6
Sm	1.5	4.5	3.4	2.6	1	4.1	3.2	5.1	2.8	2.9	2.7	2.5	3.3
Eu	0.5	1.2	1	1.1	<0.5	0.9	1.4	0.5	0.9	1	0.99	1.14	1.23
Gd	1.2	3	3.7	3.8	1	2.4	3.7	3.1	3.4	3.9	2.83	3.11	3.84
Tb	0.2	0.5	0.7	0.6	0.2	0.3	0.6	0.5	0.6	0.7	0.54	0.5	0.68
Dy	1	2.5	3.6	4.2	1.1	1.5	4	2.9	3.8	4.3	3.39	3.61	4.39
Ho	0.2	0.5	0.9	1	0.2	0.3	0.8	0.6	0.8	0.9	0.83	0.75	0.88
Er	0.7	1.5	2.9	2.9	1	0.9	2.4	2	2.5	2.7	2.38	2.21	2.78
Yb	0.8	1.2	2.8	2.8	1.4	0.7	2.2	2.9	2.5	2.5	2.5	2	2.63
Lu	0.1	0.2	0.4	0.4	0.2	0.1	0.4	0.5	0.4	0.4	0.32	0.31	0.38
Eu/Eu*	1.07	1.02	0.84	1.03	0.75	0.87	1.28	0.40	0.85	0.90	1.09	1.25	1.05
(La/Yb) _N	9.62	12.56	3.06	0.99	3.18	28.00	3.34	7.83	3.15	1.81	1.23	1.29	2.04
(La/Sm) _N	4.43	2.98	2.32	0.96	3.95	4.40	2.15	4.13	2.55	1.45	1.04	0.95	1.5

Rare Earth spectra normalized to the primitive mantle (McDonough and Sun, 1995) show a flat profile for basalts and this translates into low fractionation as shown by LREE/HREE ratios $(La/Yb)_N = 0.99-1.81$. In contrast, the spectra of basaltic andesites, dacites and andesites show low enrichment in light rare earths (LREE). However, in the calc-alkaline series, andesite shows a high fractionation rate with sufficiently high LREE/HREE ratios $(La/Yb)_N = 12.56$ and $(La/Sm)_N = 2.98$ (Fig.5-D).

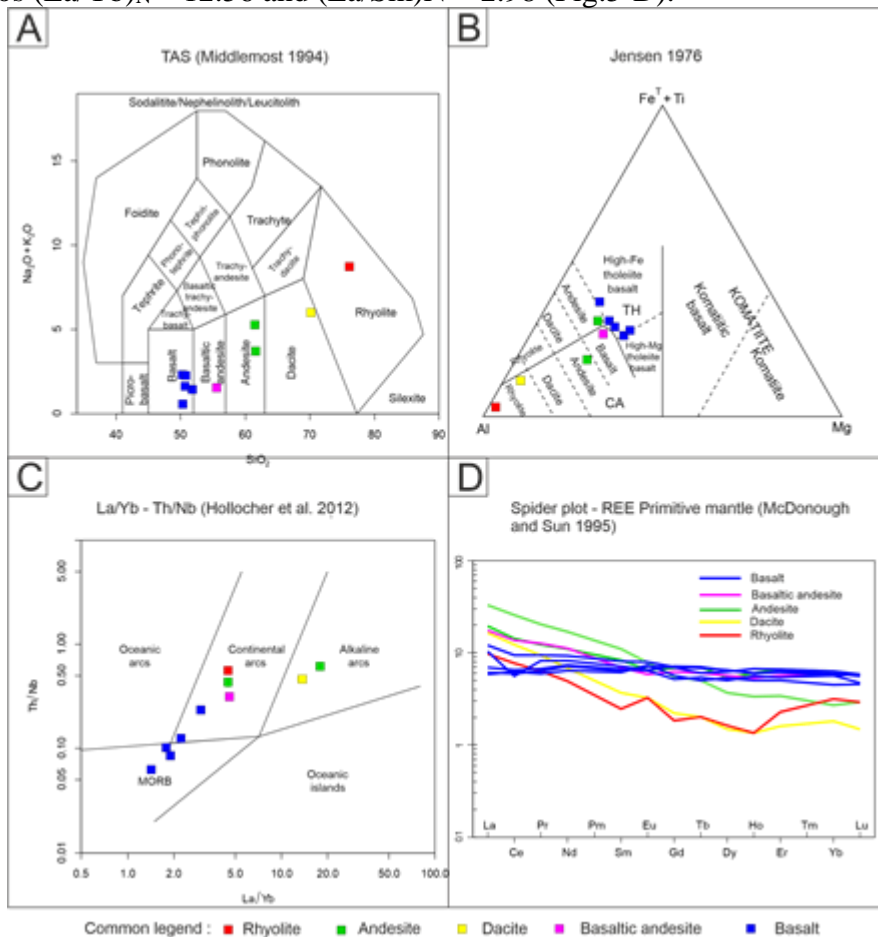


Figure 05. (A) Representation of volcanic formations in the diagram by Middlemost, (1994). (B) Magmatic series discrimination diagram by Jensen, (1976). (C) La/Yb vs Th/Nb binary diagram of geotectonic discrimination (Hollocher et al., 2012). (D) Rare Earth spectra of volcanic formations in the study area normalized to the Primeval Mantle (McDonough and Sun 1995).

4.3 The nature of the geochemical anomaly sets delineated

Litho-geochemistry essentially distinguishes two sets of geochemical anomalies depending on the family to which the indexed rocks belong: (i) a basic type located in the mafic to intermediate volcanic formations of the Boromo greenstone belt, and (ii) an acid type located in the granitoids with

high silica (62.8 to 74.69%) and potassium (2.04 to 5.54%) contents. The basic type is relatively enriched in metals. The average gold (Au) content is 8.5 ppb in the greenstone formations versus 1.35 ppm in the granitoids, while the average Cu content is 36.15 ppb in the greenstone belt formations versus 10.1 ppb in the granitoids. Overall, the basic type is enriched in Au, Cr, Co, Cu, Ni and Zn compared with the acidic type (Fig.6). From the point of view of metal anomaly distribution, we note that Cr and Ni are specifically much more represented in the ultramafic volcanic formations of the belt and almost absent in granitic facies. They are found in contact zones with the volcanic formations of the Birimian belt and in shear zones where deformation allows mineralizing fluids to remobilize towards these granitic formations. On the other hand, Pb is more prevalent in the granitoids, with levels ranging from 5.5 to 28.6 ppb, but is low or non-existent in the volcanic formations of the greenstone belt.

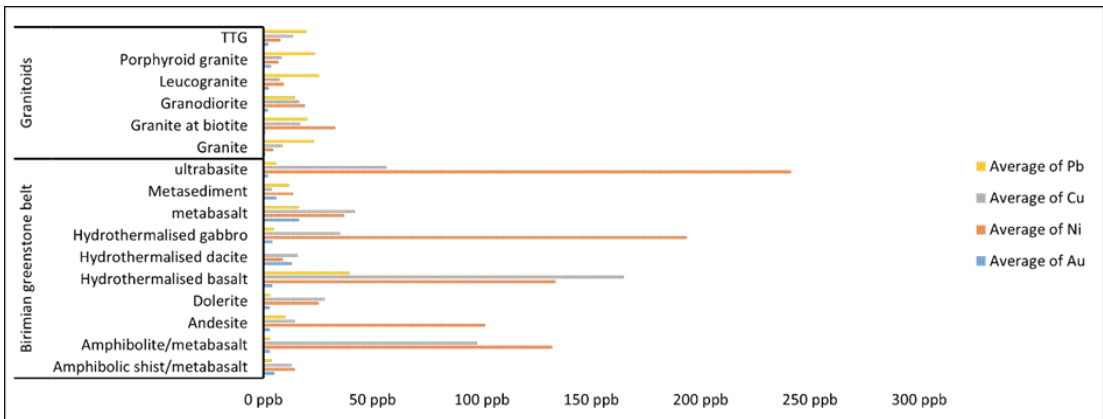


Figure 6. Histogram of average metal content in the main geological formations

5. Discussion

The Birimian formations host several gold deposits considered to be orogenic gold deposits (Milési et al., 1989, 1992; Groves et al., 1998; Markwitz et al., 2016; Goldfarb et al., 2017; Masurel et al., 2021). Most of these deposits are hydrothermal, i.e. linked to the circulation of fluids located in structural faults (Groves et al., 1998). They are mostly syn- to tardi-tectonic (Milési et al., 1989, 1992; Bourges et al., 1998; Markwitz et al., 2016; Goldfarb et al., 2017; Masurel et al., 2021). In fact, mapping and mineral exploration work in the central-western region of Burkina Faso show mostly vein-type mineralization with quartz veins and sulfides. In the discussion that follows, we first discuss the origin of the mineralized sediments and the metal fertility of the formations surrounding these sediments. We then examine the different occurrences of mineralization in the main zones.

5.1 Probable origin of stream sediments

Stream sediment data show a pronounced enrichment of Au, Cu, Ni and Zn in clay-type samples, to the detriment of sandy-type samples. The sandy-clay type is low in metal mineralization. This is mainly due to the fact that most of the samples tested in the greenstone belt formations were not only rich in gold, Cu, Ni and Zn, but also yielded clay-type sediments through supergene alteration. However, the origin of the clays is not clearly established, as they may originate from greenstone belt formations and/or granitoid formations. Studies of granite formations show that they weather under the influence of climate to produce sands and clays (Cullers, 1988). However, several studies have already demonstrated the importance of stream sediment sample grain size for prospecting (Ndome Effoudou-Priso et al., 2014; Manuela Vinha G. Silva et al., 2016; Shruti et al., 2017; Sorokina, 2019). Indeed, fine fractions such as clays/limons in sediments are capable of concentrating and transporting many elements associated with most types of mineral deposits (Chandrajith et al., 2001; Manuela Vinha G. Silva et al., 2016; Martinčić et al., 1990; Melo and Fletcher, 1999; Young et al., 2013). In Sri Lanka, for example, the work of Chandrajith et al. (2001) indicates that grain size fractions below 177 μm are considered a preferable fraction to coarse (sand) for geochemical exploration studies of stream sediments in tropical terrains with high content of gold and various other metals.

Analysis of stream sediment data for immobile major elements and trace elements such as Ti, Fe, Al, Th, Sc, Co and Zr are good indicators for investigating the source of sediments (Taylor and McLennan, 1985). $\text{Al}_2\text{O}_3/\text{TiO}_2$ ratios are most often exploited to search for source rock, due to the fact that they are considered immobile elements during surface weathering (Hayashi et al., 1997; He et al., 2010; Shao et al., 2016). The Al /Ti ratio increases proportionally with Si (Hayashi et al., 1997). According to Hayashi et al. (1997), $\text{Al}_2\text{O}_3/\text{TiO}_2$ ratios increase from 3 to 8, 821 and 2170 respectively in mafic, intermediate and felsic igneous source rocks. In the present study, $\text{Al}_2\text{O}_3/\text{TiO}_2$ ratios ranged from 4 to 14 in anomaly zone one (01) for samples with high Au grades. In anomaly zone two (02), $\text{Al}_2\text{O}_3/\text{TiO}_2$ ratios range from 6 to 14, also for high Au grades. These results show that the clayey sediments rich in gold and other metals originate mainly from the basic to intermediate magmatic formations of the Birimian belt (Fig.7).

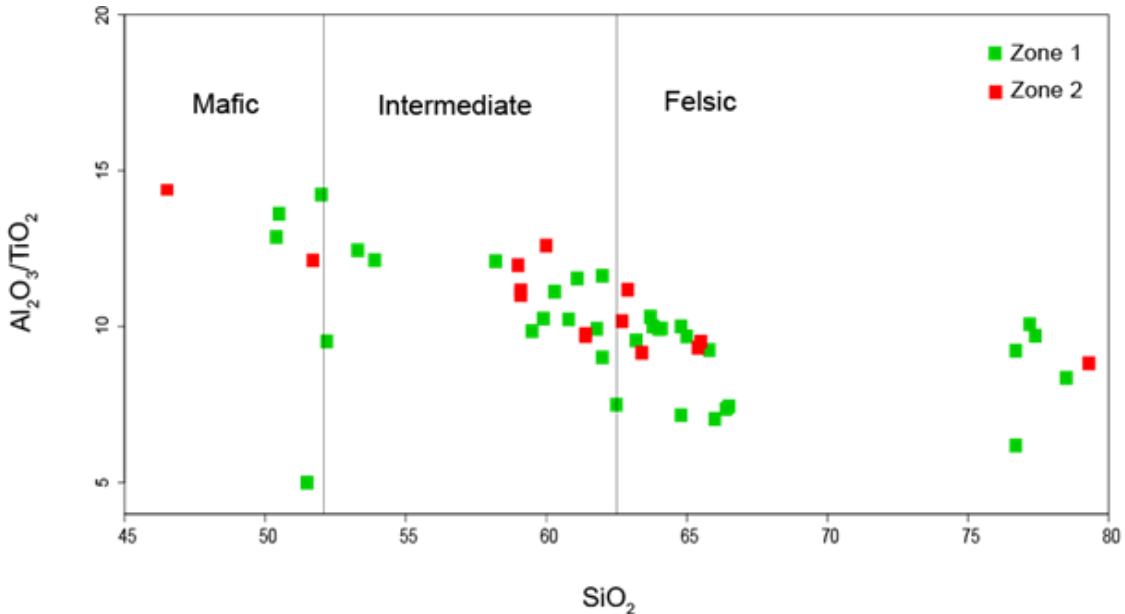


Figure 7. Binary diagram illustrating Al_2O_3/TiO_2 vs. SiO_2 ratios of stream sediments in Anomaly Zones 1 and 2 from Le Bas et al. (1986)

In addition to the high gold, Cr and Ni contents in stream sediment samples, anomaly zones one (01) and two (02) delineated confirm this provenance trend. Indeed, ultrabasic rocks produce sediments with high Cr and Ni contents, while low Cr concentrations indicate a felsic origin (Wrafter and Graham, 1989; Garver et al., 1996; Armstrong-Altrin et al., 2004). Cr and Ni concentrations are particularly high in anomaly zone two (02), with Cr/Ni ratios ranging from 1.16 to 2.6 (see Table II).

5.2 Fertile gold formations

The geodynamic context of the basaltic formations of the West African Craton (WAC) is defined by two groups of authors. A first group of authors (Zonou et al., 1985; Ama Salah et al., 1996; Béziat et al., 2000; Baratoux et al., 2011; Eglinger et al., 2017; Wane et al., 2018) propose that the WAC basalts formed in a mid-ocean rift or island arc context. The second group of authors propose an oceanic shelf context with mantle plume activity (Abouchami et al., 1990; Boher et al., 1992; Tayllor et al., 1992; Pouclet et al., 2006, Lompo, 2009; Augustin and Gaboury, 2017). Lompo (2009) defined three types of tholeiites for the WAC formations ranging from PTH1 to PTH3. For the geodynamic context, he proposes an oceanic basin formed by subsidence. In view of what has been said above, we propose that the basalts of the Tenado region are linked to emplacement in an oceanic plateau context in connection with mantle plume activity; as this type of basalt displays

chondrite-normalized rare-earth flat spectra similar to those of the West African craton (Lompo, 2009, Augsutin and Gaboury, 2017).

This type of basalt is a primary source of gold and various metals (Augustin and Gaboury, 2017; Ouyia et al., 2022). In the same vein, earlier work by Chevremont et al. (2003) on the Koudougou square degree in the Perkoa locality showed that in the anomalies of the basaltic-type assemblage (basalt), Au, Cu and Mg enrichment distinguishes it from other volcanic formations (Fig. 6). This fertility of basalt in gold and other metals has also been reported in the nearby Houndé greenstone belt (Augustin and Gaboury, 2017). In the previous paragraph, we showed that gold-rich clay sediments are derived from basic (basalt) to intermediate (andesite, dacite) rocks. What's more, our litho-geochemical data show that basalts and intermediate rocks are fertile in gold and various metals. Based on all this, we propose that the source of gold in sediments is related to basic to intermediate rocks.

5.3 Evidence of zones with high gold and base metal potential

a) Anomaly zone one (01)

This zone contains four (04) mapped gold showings in the localities of Kelsio, Zoula, Poa and Dyoro (Fig.8). In addition to these gold showings, Perkoa is a zinc mine. The Perkoa deposit is a polymetallic Zn-Ag volcanogenic sulfide cluster (VMS) (Napon, 1988; Ouedraogo, 1989; Milési et al., 1989; Schwartz and Melcher, 2001, 2003). In contrast, in the four (04) gold showings cited, mineralization is mainly vein-type and located in the shear zone. It takes the form of disseminated mineralization with a strong presence of sulfides in silicified zones (Ouedraogo, 1989; Kabore et al., 1989; Lompo, 1991; Chevremont et al., 2003). In all four (4) zones, gold is mined artisanally (orpaillage) in quartz veinlets/veins along a N-S to NE-SW trending structure in highly sheared metavolcanic and metasedimentary host rocks.

b) Anomaly zone two (02)

A variety of metal showings (Cu, Ni and Au) were recorded in this anomaly area. A total of five (05) showings were recorded, covering the localities of Kwademan, Baguimo, Bérédo, Bonga and Baganapou (Fig.8). The Bonga showing shows Ni mineralization in a zone of supergene alteration in lateritic and bauxitic formations (Kabore et al., 1989; Ouedraogo, 1989). In contrast, the Kwademen deposit shows occurrences of gold (Ouedraogo, 1989; Lompo et al., 1991) and base metals (Cu and Mn) (Lompo, 1991; Ilboudo, 2006; Ilboudo et al., 2015). At Kwademen, prospecting for gold has shown that mineralization is linked to cataclastic quartz veins with free gold, gold-pyrite, arsenopyrite and chalcopyrite, mainly submeridian in orientation (Ouedraogo, 1989; Kabore et al., 1989; Lompo, 1991; Chevremont et al.,

2003). Gold mineralization at Baguïomo occurs as pyrite-gold quartz veins or as disseminated pyrite-gold rock (Ouiya et al., 2024). The Bérédo and Baganapou gold deposits occur as vein-type mineralization, with gold finely disseminated, rarely as Stockwerk in strongly hydrothermalized host rocks. Alteration in these zones varies (silicification, sericitization, etc.), but can be much more complex in faulted contact zones with granitoids. The main shear zones show similar orientations to the first anomaly area. The main gold mining activity is gold panning, but in localities such as Baguïomo, Tiekouyou and Karabole it appears to be under-explored.

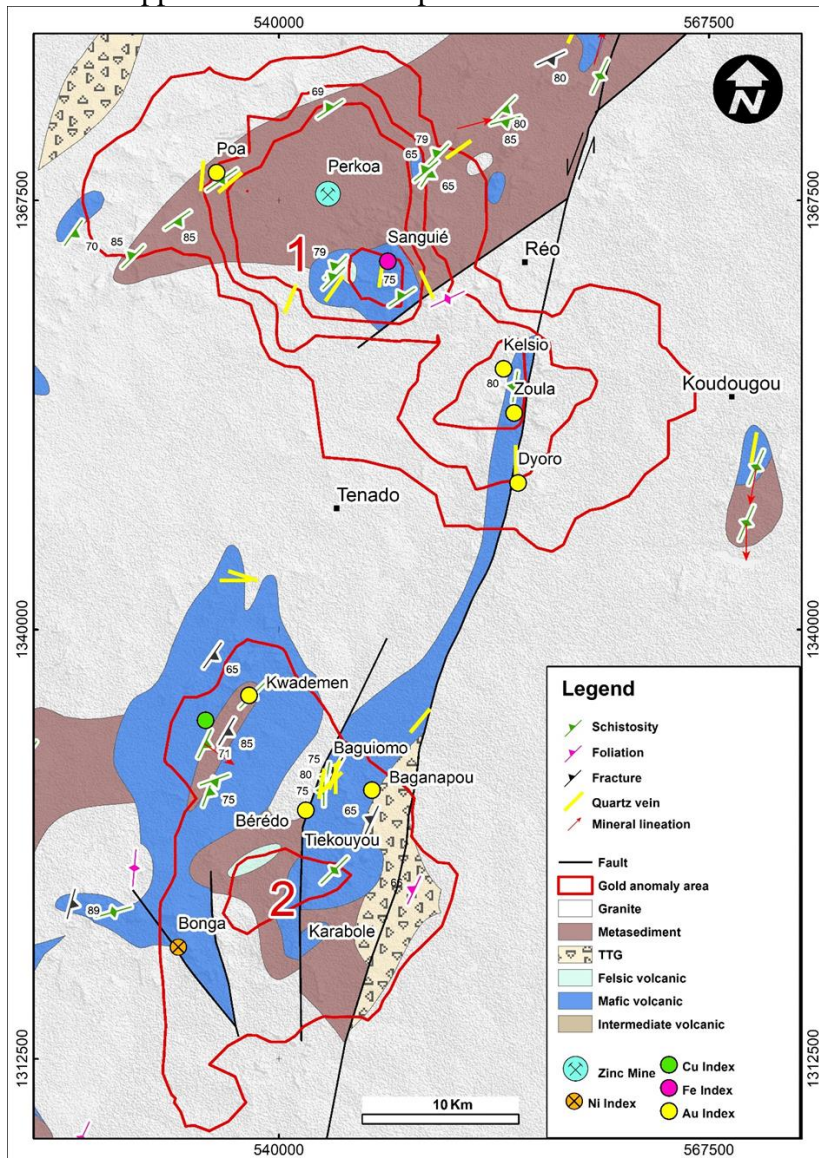


Figure 8. Structural map and mineral showings

Conclusion

The combination of gold content in stream sediments and litho-geochemical data has enabled us to highlight two areas of gold (Au) and miscellaneous metal anomalies. Gold content in stream sediments is mainly influenced by that of the source rock from which it is derived. High gold anomalies are found in both clayey and sandy sediments. Clayey sediments are thought to originate from basic (basalt) to intermediate (andesite-dacite) rocks, while gold-poor sandy sediments are thought to originate from granitoids.

The basic to intermediate rocks are fertile for primary gold. Anomaly zone one (01) in the northern part of the study area and anomaly zone two (02) in the southern part of the study area show occurrences of mainly gold and various metals (Zn, Cu, Ni). The evidence of these two zones thus delineated constitutes zones of major interest for gold (Au) prospecting. These zones are of greatest interest when they occur in shear zones or in close proximity to host formations affected by hydrothermal alteration. Anomaly zone two (02) is located in a shear zone.

Acknowledgements

Our first thanks go to BUMIGEB (Bureau of Mines and Geology of Burkina Faso), which provided us with geochemical data for this study. The geochemical work was acquired during the SYSMIN 2003 project. This work is part of my doctoral thesis at Joseph KI-ZERBO University.

Conflict of Interest: The authors reported no conflict of interest.

Data Availability: All of the data are included in the content of the paper.

Funding Statement: The authors did not obtain any funding for this research.

References:

1. Abdolmaleki, M., Mokhtari, A.R., Akbar, S., Alipour-Asll, M., Carranza, E.J.M., 2014. Catchment basin analysis of stream sediment geochemical data: Incorporation of slope effect. *Journal of Geochemical Exploration* 140, 96–103.
<https://doi.org/10.1016/j.gexplo.2014.02.029>
2. Abouchami, W., Boher, M., Michard, A., Albarede, F., 1990. A major 2.1 Ga event of mafic magmatism in west Africa : An Early stage of crustal accretion. *J. Geophys. Res.* 95, 17605.
<https://doi.org/10.1029/JB095iB11p17605>
3. Armstrong-Altrin, J.S., Lee, Y.I., Verma, S.P., Ramasamy, S., 2004. *Geochemistry of Sandstones from the Upper Miocene Kudankulam*

- Formation, Southern India: Implications for Provenance, Weathering, and Tectonic Setting. *Journal of Sedimentary Research* 74, 285–297. <https://doi.org/10.1306/082803740285>
4. Augustin, J., Gaboury, D., 2017. Paleoproterozoic plume-related basaltic rocks in the Mana gold district in western Burkina Faso, West Africa : Implications for exploration and the source of gold in orogenic deposits. *Journal of African Earth Sciences* 129, 17–30. <https://doi.org/10.1016/j.jafrearsci.2016.12.007>
 5. Baratoux, L., Metelka, V., Naba, S., Jessell, M.W., Grégoire, M., Ganne, J., 2011. Juvenile Paleoproterozoic crust evolution during the Eburnean orogeny (~2.2–2.0Ga), western Burkina Faso. *Precambrian Research* 191, 18–45. <https://doi.org/10.1016/j.precamres.2011.08.010>
 6. Bas, M.J.L., Maitre, R.W.L., Streckeisen, A., Zanettin, B., IUGS Subcommission on the Systematics of Igneous Rocks, 1986. A Chemical Classification of Volcanic Rocks Based on the Total Alkali-Silica Diagram. *Journal of Petrology* 27, 745–750. <https://doi.org/10.1093/petrology/27.3.745>
 7. Bessoles, B., 1977. Géologie de l’Afrique : le craton Ouest Africain. *Mém. B.R.G.M., Paris* 88, 403p.
 8. Béziat, D., Bourges, F., Debat, P., Lompo, M., Martin, F., Tollon, F., 2000. A Paleoproterozoic ultramafic-mafic assemblage and associated volcanic rocks of the Boromo greenstone belt: Fractionates originating from island-arc volcanic activity in the West African craton. *Precambrian Research* 101, 25–47. [https://doi.org/10.1016/S0301-9268\(99\)00085-6](https://doi.org/10.1016/S0301-9268(99)00085-6)
 9. Béziat, D., Dubois, M., Debat, P., Nikiéma, S., Salvi, S., Tollon, F., 2008. Gold metallogeny in the Birimian craton of Burkina Faso (West Africa). *Journal of African Earth Sciences* 50, 215–233. <https://doi.org/10.1016/j.jafrearsci.2007.09.017>
 10. Boher, M., Abouchami, W., Michard, A., Albarede, F., Arndt, N.T., 1992. Crustal growth in West Africa at 2.1 Ga. *J. Geophys. Res.* 97, 345. <https://doi.org/10.1029/91JB01640>
 11. Bonhomme, M., 1962. Contribution à l’étude géochronologique de la plate-forme de l’Ouest Africain. *Annals de la Faculté des Sciences de Université de ClermontFerrand Géol. Minéral* 5 62.
 12. Bourges, F., Debat, P., Tollon, F., Munoz, M., Ingles, J., 1998. The geology of the Taparko gold deposit, Birimian greenstone belt, Burkina Faso, West Africa, *Mineralium Deposita* 591–605.
 13. Carranza, E.J.M., 2010. Mapping of anomalies in continuous and discrete fields of stream sediment geochemical landscapes. *GEEA* 10, 171–187. <https://doi.org/10.1144/1467-7873/09-223>

14. Castaing, C., Billa, M., Milesi, J.P., Thieblemont, D., Le Metour, J., Egal, E., Donzeau, M., Guerrot, C., Cocherie, A., Chevremont, P., Tegye, M., Itard, Y., Zida, B., Ouedraogo, I., Kote, S., Kabore, B.E., Ouedraogo, C., Ki, J.C., Zunino, C., 2003. Notice explicative de la Carte géologique et minière du Burkina Faso à 1/1 000 000.
15. Chandrajith, R., Dissanayake, C.B., Tobschall, H.J., 2001. Application of multi-element relationships in stream sediments to mineral exploration: a case study of Walawe Ganga Basin, Sri Lanka. *Applied Geochemistry* 16, 339–350. [https://doi.org/10.1016/S0883-2927\(00\)00038-X](https://doi.org/10.1016/S0883-2927(00)00038-X)
16. Chevremont, P., Donzeau, M., Le Metour, J., Egal, E., Castaing, C., Thieblemont, D., Tegye, M., Guerrot, C., Billa, M., Itard, Y., Delpont (BRGM), G., Ki, J.-C., Zunino (ANTEA), C., 2003. Notice explicative de la carte géologique à 1/200 000 Feuille ND-30-IV KOUDOUGOU 1ère édition, 76.
17. Cullers, R., 1988. Mineralogical and chemical changes of soil and stream sediment formed by intense weathering of the Danburg granite, Georgia, U.S.A. *Lithos* 21, 301–314. [https://doi.org/10.1016/0024-4937\(88\)90035-7](https://doi.org/10.1016/0024-4937(88)90035-7)
18. Dahl, R., Giovenazzo, D., Hein, K.A.A., Ouédraogo, C., Séjourné, S., Ouedraogo, A., Ouédraogo, P.I., Sountra, Y., Kambou, A., Coulibaly, G.K., Nassa, O., Nassa, N., Djiguemde, S., Hema, K.A.A., Bagoro, F., Sidibé, G., 2018. Carte de synthèse géologique, structurale et des substances minérales du Burkina Faso à 1/1000000.
19. Darehshiri, A., Panji, M., Mokhtari, A.R., 2015. Identifying geochemical anomalies associated with Cu mineralization in stream sediment samples in Gharachaman area, northwest of Iran. *Journal of African Earth Sciences* 110, 92–99. <https://doi.org/10.1016/j.jafrearsci.2015.06.009>
20. Doumbia, S., Pouclet, A., Kouamelan, A., Peucat, J.J., Vidal, M., Delor, C., 1998. Petrogenesis of juvenile-type Birimian (Paleoproterozoic) granitoids in Central Côte-d’Ivoire, West Africa: geochemistry and geochronology. *Precambrian Research* 87, 33–63. [https://doi.org/10.1016/S0301-9268\(97\)00201-5](https://doi.org/10.1016/S0301-9268(97)00201-5)
21. Eglinger, A., Thébaud, N., Zeh, A., Davis, J., Miller, J., Parra-Avila, L.A., Loucks, R., McCuaig, C., Belousova, E., 2017. New insights into the crustal growth of the Paleoproterozoic margin of the Archean Kéména-Man domain, West African craton (Guinea): Implications for gold mineral system. *Precambrian Research* 292, 258–289. <https://doi.org/10.1016/j.precamres.2016.11.012>
22. Feybesse, J.-L., Billa, M., Guerrot, C., Duguey, E., Lescuyer, J.-L., Milesi, J.-P., Bouchot, V., 2006. The paleoproterozoic Ghanaian

- province: Geodynamic model and ore controls, including regional stress modeling. *Precambrian Research* 149, 149–196.
<https://doi.org/10.1016/j.precamres.2006.06.003>
23. Feybesse, J.-L., Milesi, J.-P., Ouédraogo, M.F., Prost, A., 1990. La « ceinture » protérozoïque inférieure de Boromo-Goren Burkina Faso: un exemple d'interférence entre deux phases transcurrentes éburnéennes. *C. R. Acad. Sci. Paris*, 310 1353–1360.
 24. Franceschi, G., Ouédraogo, B., 1982. Prospection minière détaillée sur l'indice Pb-Zn-Ag dans le secteur de Perkoa (NW Réo) (Rap. tech. 1 and 2), (UPV 74/004, Haute-Volta, BUVOGMIPNUD, inédit).
 25. Ganne, J., Gerbault, M., Block, S., 2014. Thermo-mechanical modeling of lower crust exhumation—Constraints from the metamorphic record of the Palaeoproterozoic Eburnean orogeny, West African Craton. *Precambrian Research* 243, 88–109.
<https://doi.org/10.1016/j.precamres.2013.12.016>
 26. Garver, J.I., Royce, P.R., Smick, T.A., 1996. Chromium and Nickel in Shale of the Taconic Foreland: A Case Study for the Provenance of Fine-Grained Sediments with an Ultramafic Source. *SEPM JSR Vol. 66*.
<https://doi.org/10.1306/D42682C5-2B26-11D7-8648000102C1865D>
 27. Gasquet, D., Barbey, P., Adou, M., Paquette, J.L., 2003. Structure, Sr–Nd isotope geochemistry and zircon U–Pb geochronology of the granitoids of the Dabakala area (Côte d'Ivoire): evidence for a 2.3 Ga crustal growth event in the Palaeoproterozoic of West Africa? *Precambrian Research* 127, 329–354. [https://doi.org/10.1016/S0301-9268\(03\)00209-2](https://doi.org/10.1016/S0301-9268(03)00209-2)
 28. Giovenazzo, D., Séjourné, S., Hein, K.A.A., Jébrak, M., Dahl, R., Ouedraogo, C., Ouedraogo, F.O., Wenmega, U., 2018. Notice explicative de la Carte géologique et minière du Burkina Faso à 1/1 000 000. BUMIGEB (Burkina Faso) 52.
 29. Goldfarb, R.J., André-Mayer, A.-S., Jowitt, S.M., Mudd, G.M., 2017. West Africa: The World's Premier Paleoproterozoic Gold Province. *Economic Geology* 112, 123–143.
<https://doi.org/10.2113/econgeo.112.1.123>
 30. Groves, D.I., Goldfarb, R.J., Gebre-Mariam, M., Hagemann, S.G., Robert, F., 1998. Orogenic gold deposits: A proposed classification in the context of their crustal distribution and relationship to other gold deposit types. *Ore Geology Reviews* 13, 7–27.
[https://doi.org/10.1016/S0169-1368\(97\)00012-7](https://doi.org/10.1016/S0169-1368(97)00012-7)
 31. Hayashi, K.-I., Fujisawa, H., Holland, H.D., Ohmoto, H., 1997. Geochemistry of ~1.9 Ga sedimentary rocks from northeastern

- Labrador, Canada. *Geochimica et Cosmochimica Acta* 61, 4115–4137.
[https://doi.org/10.1016/S0016-7037\(97\)00214-7](https://doi.org/10.1016/S0016-7037(97)00214-7)
32. He, Z., Xu, X., Zou, H., Wang, X., Yu, Y., 2010. Geochronology, petrogenesis and metallogeny of Piaotang granitoids in the tungsten deposit region of South China. *Geochem. J.* 44, 299–313.
<https://doi.org/10.2343/geochemj.1.0073>
33. Hirdes, W., Davis, D.W., Lüdtke, G., Konan, G., 1996. Two generations of Birimian (Paleoproterozoic) volcanic belts in northeastern Côte d'Ivoire (West Africa): consequences for the 'Birimian controversy.' *Precambrian Research* 80, 173–191.
[https://doi.org/10.1016/S0301-9268\(96\)00011-3](https://doi.org/10.1016/S0301-9268(96)00011-3)
34. Hollocher, K., Robinson, P., Walsh, E., Roberts, D., 2012. Geochemistry of amphibolite-facies volcanics and gabbros of the Støren Nappe in extensions west and southwest of Trondheim, western gneiss region, Norway: A key to correlations and paleotectonic settings. *American Journal of Science* 312, 357–416.
<https://doi.org/10.2475/04.2012.01>
35. Ilboudo, H., 2015. A stratiform (Cu-Zn±Pb) sulphide and gold occurrences in the Kwademen Birimian system (Burkina Faso, West Africa). *Asian Academic Research Journal of Multidisciplinary* 2, 23p.
36. Ilboudo, H., 2006. Analyse pétrographique et métallographique des sondages carottés du prospect de Kwademen (Centre Ouest du Burkina Faso) (Mémoire de DEA). Université de Ouagadougou, Ouagadougou.
37. Jensen, L.S., 1976. A new cation plot for classifying subalkalic volcanic rocks. 1–21.
38. Junner, N.R., 1940. Geology of the Gold Coast and western Togoland (with revised geological map). *Gold Coast Geological Survey Bulletin* 11 1–40p.
39. Kabore, J., Mathez, G., Ouedraogo, M.F., Sattran, V., 1989. Prospection géochimique dans le centre et le nord-ouest du Burkina Faso. *Journal of Geochemical Exploration* 32, 429–435.
[https://doi.org/10.1016/0375-6742\(89\)90088-5](https://doi.org/10.1016/0375-6742(89)90088-5)
40. Kitson, A.E., 1918. Annual Report n°948. *Gold Coast Geological Survey for 1916/17*, Accra.
41. Lompo, M., 2009. Geodynamic evolution of the 2.25-2.0 Ga Palaeoproterozoic magmatic rocks in the Man-Leo Shield of the West African Craton. A model of subsidence of an oceanic plateau. *Geological Society, London, Special Publications* 323, 231–254.
<https://doi.org/10.1144/SP323.11>
42. Lompo, M., 1991. Etude géologique et structurale des séries birimiennes de la région de kwademen-burkina faso-afrique de l'ouest.

43. Lompo, M., Caby, R., Robineau, B., 1991. Evolution structurale du Birimien au Burkina-Faso: exemple de la ceinture de Boromo–Goren dans le secteur de Kwademen (Afrique de l’Ouest). *Comptes Rendus de l’Académie des Sciences de Paris Série II* 313, 945–950.
44. Manuela Vinha G. Silva, M., M.S. Cabral Pinto, M., Carvalho, P.C.S., 2016. Major, trace and REE geochemistry of recent sediments from lower Catumbela River (Angola). *Journal of African Earth Sciences* 115, 203–217. <https://doi.org/10.1016/j.jafrearsci.2015.12.014>
45. Markwitz, V., Hein, K.A.A., Jessell, M.W., Miller, J., 2016. Metallogenic portfolio of the West Africa craton. *Ore Geology Reviews* 78, 558–563. <https://doi.org/10.1016/j.oregeorev.2015.10.024>
46. Martinčić, D., Kwokal, Ž., Branica, M., 1990. Distribution of zinc, lead, cadmium and copper between different size fractions of sediments II. The Krka River Estuary and the Kornati Islands (Central Adriatic Sea). *Science of The Total Environment* 95, 217–225. [https://doi.org/10.1016/0048-9697\(90\)90066-4](https://doi.org/10.1016/0048-9697(90)90066-4)
47. Masurel, Q., Eglinger, A., Thébaud, N., Allibone, A., André-Mayer, A.-S., McFarlane, H., Miller, J., Jessell, M., Aillères, L., Vanderhaeghe, O., Salvi, S., Baratoux, L., Perrouty, S., Begg, G., Fougereuse, D., Hayman, P., Wane, O., Tshibubudze, A., Parra-Avila, L., Kouamélan, A., Amponsah, P.O., 2021. Paleoproterozoic gold events in the southern West African Craton: review and synopsis. *Miner Deposita*. <https://doi.org/10.1007/s00126-021-01052-5>
48. McDonough, W.F., Sun, S. -s., 1995. The composition of the Earth. *Chemical Geology* 120, 223–253. [https://doi.org/10.1016/0009-2541\(94\)00140-4](https://doi.org/10.1016/0009-2541(94)00140-4)
49. Melo, G., Fletcher, W.K., 1999. Dispersion of gold and associated elements in stream sediments under semi-arid conditions, northeast Brazil. *Journal of Geochemical Exploration* 67, 235–243. [https://doi.org/10.1016/S0375-6742\(99\)00053-9](https://doi.org/10.1016/S0375-6742(99)00053-9)
50. Metelka, V., Baratoux, L., Naba, S., Jessell, M.W., 2011. A geophysically constrained litho-structural analysis of the Eburnean greenstone belts and associated granitoid domains, Burkina Faso, West Africa. *Precambrian Research* 190, 48–69. <https://doi.org/10.1016/j.precamres.2011.08.002>
51. Middlemost, E.A.K., 1994. Naming materials in the magma/igneous rock system. *Earth-Science Reviews* 37, 215–224. [https://doi.org/10.1016/0012-8252\(94\)90029-9](https://doi.org/10.1016/0012-8252(94)90029-9)
52. Milési, J.-P., Feybesse, J.-L., Ledru, P., Dommaget, A., Ouédraogo, M.F., Marcoux, E., Prost, A., Vinchon, C., Sylvain, J.-P., Johan, V., Tegye, M., Calvez, J.-Y., Lagny, P., 1989. Les minéralisations

- aurifères de l’Afrique de l’Ouest. *Chronique Recherche Minière*, n°497 3–98.
53. Milesi, J.-P., Feybesse, J.-L., Pinna, P., Deschamps, Y., Kampunzu, A.B., Muhongo, S., Lescuyer, J.L., Le Goff, E., Delor, C., Ralay, F., Henry, C., 2004. Géologie et principaux gisements d’Afrique - Carte et SIG à 1/10 000 000. Abstracts Volume 20th Colloquium of African Geology in Orleans, France 128p.
 54. Milési, J.-P., Ledru, P., Feybesse, J.-L., Dommange, A., Marcoux, E., 1992. Early Proterozoic ore deposits and tectonics of the Birimian orogenic belt, West Africa. *Precambrian Research - PRECAMBRIAN RES* 58, 305–344. [https://doi.org/10.1016/0301-9268\(92\)90123-6](https://doi.org/10.1016/0301-9268(92)90123-6)
 55. Napon, S., 1988. Le gisement d’amas sulfuré (Zn-Ag) de Perkoa dans la Pvince du Sangyé (Burkina Faso, Afrique de l’Ouest) : Cartographie, Etude pétrographique, géochimique et métallogénique. Thèse Doc. Univ. Franche-Comté, France 309.
 56. Ndome Effoudou-Priso, E., Onana, V.L., Boubakar, L., Beyala, V.K.K., Ekodeck, G.E., 2014. Relationships between major and trace elements during weathering processes in a sedimentary context: Implications for the nature of source rocks in Douala, Littoral Cameroon. *Geochemistry* 74, 765–781. <https://doi.org/10.1016/j.chemer.2014.05.003>
 57. Noa Tang, S.D., Ntsama Atangana, J., Onana, V.L., 2020. Mineralogy and geochemistry of alluvial sediments from the Kadey plain, eastern Cameroon: Implications for provenance, weathering, and tectonic setting. *Journal of African Earth Sciences* 163, 103763. <https://doi.org/10.1016/j.jafrearsci.2020.103763>
 58. Ouedraogo, F.O., 1988. The Kwademen Gold Deposit : a polymorphic mineralization within a Precambrian (Birrimian) greenstone belt in Burkina Faso, West Africa: a Case History. *AusIMM, Perth, Symposia Series*.
 59. Ouedraogo, M.F., 1989. Eléments de synthèse sur l’évolution géostructurale et la métallogénie de la ceinture birrimienne de Boromo (Protérozoïque inférieur, Burkina Faso). Thèse Doct. Sci., Univ. Orléans, France 115p.
 60. Ouyi, P., Tarnagda, A.F., Fozing, M.E., 2024. Characteristics of Gold Mineralization at the Baguiomo Gold Panning Site, Koudougou Region, Burkina Faso, West Africa. *OJG* 14, 1–18. <https://doi.org/10.4236/ojg.2024.141001>
 61. Ouyi, P., Yaméogo, A.O., Ilboudo, H., Naba, S., 2022. Implication of Paleoproterozoic Basalt Fertility Related to Mantle Plume Activity in Nassara Gold Mineralization (Burkina Faso, West Africa). *OJG* 12, 1013–1031. <https://doi.org/10.4236/ojg.2022.1211048>

62. Pouclet, A., Doumbia, S., Vidal, M., 2006. Geodynamic setting of the Birimian volcanism in central Ivory Coast (western Africa) and its place in the Palaeoproterozoic evolution of the Man Shield. *Bulletin de la Société Géologique de France* 177, 105–121.
<https://doi.org/10.2113/gssgfbull.177.2.105>
63. Salah, I.A., Liegeois, J.-P., Pouclet, A., 1996. Evolution d'un arc insulaire océanique birimien précoce au Liptako nigérien (Sirba): géologie, géochronologie et géochimie. *Journal of African Earth Sciences* 22, 235–254. [https://doi.org/10.1016/0899-5362\(96\)00016-4](https://doi.org/10.1016/0899-5362(96)00016-4)
64. Schwartz, M.O., Melcher, F., 2003. The Perkoa Zinc Deposit, Burkina Faso. *Economic Geology* 98, 1463–1485.
<https://doi.org/10.2113/gsecongeo.98.7.1463>
65. Schwartz, M.O., Melcher, F., 2001. The geology of the Perkoa zinc deposit, Burkina Faso. Workshop VMS potential in the Birimian. BGR/BUMIGEB, Ouagadougou.
66. Shao, L., Cao, L., Pang, X., Jiang, T., Qiao, P., Zhao, M., 2016. Detrital zircon provenance of the Paleogene syn-rift sediments in the northern South China Sea: PALEOGENE SOURCE OF NORTHERN SOUTH CHINA SEA. *Geochem. Geophys. Geosyst.* 17, 255–269.
<https://doi.org/10.1002/2015GC006113>
67. Shine, Y.J., Moye, C.D., Mallya, G.J., Tamambele, A.L., 2022. Generation of Geochemical Exploration Targets from Regional Stream Sediment Data Using Principal Component and Factor Ana. *Tanz. J. Sci.* 48, 668–679. <https://doi.org/10.4314/tjs.v48i3.14>
68. Shruti, V.C., Jonathan, M.P., Rodríguez-Espinosa, P.F., Nagarajan, R., Escobedo-Urias, D.C., Morales-García, S.S., Martínez-Tavera, E., 2017. Geochemical characteristics of stream sediments from an urban-volcanic zone, Central Mexico: Natural and man-made inputs. *Geochemistry* 77, 303–321.
<https://doi.org/10.1016/j.chemer.2017.04.005>
69. Sorokina, O.A., 2019. Reconstruction of Sources in River Sediments in the Lower Part of the Bureya River Based on Geochemical Indices. *Russian Journal of Pacific Geology* 13, 176–185.
<https://doi.org/10.1134/S1819714019020088>
70. Taylor, S.R., McLennan, S.M., 1985b. *The Continental Crust: Its Composition and Evolution*. Blackwell Scientific Publications 312 122, 673–674.
71. Wane, O., Liégeois, J.-P., Thébaud, N., Miller, J., Metelka, V., Jessell, M., 2018. The onset of the Eburnean collision with the Kenema-Man craton evidenced by plutonic and volcanosedimentary rock record of the Massigui region, southern Mali. *Precambrian Research* 305, 444–478. <https://doi.org/10.1016/j.precamres.2017.11.008>

72. Wrafter, J.P., Graham, J.R., 1989. Short Paper: Ophiolitic detritus in the Ordovician sediments of South Mayo, Ireland. *JGS* 146, 213–215. <https://doi.org/10.1144/gsjgs.146.2.0213>
73. Young, S.M., Pitawala, A., Ishiga, H., 2013. Geochemical characteristics of stream sediments, sediment fractions, soils, and basement rocks from the Mahaweli River and its catchment, Sri Lanka. *Geochemistry* 73, 357–371. <https://doi.org/10.1016/j.chemer.2012.09.003>
74. Yousefi, M., Carranza, E.J.M., Kamkar-Rouhani, A., 2013. Weighted drainage catchment basin mapping of geochemical anomalies using stream sediment data for mineral potential modeling. *Journal of Geochemical Exploration* 128, 88–96. <https://doi.org/10.1016/j.gexplo.2013.01.013>
75. Zonou, S., Karche, J.P., Lapierre, H., Lemoine, S., Rossy, M., Roques, M., 1985. Volcanismes tholéitique et calco-alcalin dans les formations du Birrimien supérieur de Bouroum (N.E. Du Burkina-Faso). *Comptes rendus de l'Académie des Sciences Paris*, 301.